ACS APPLIED MATERIALS & INTERFACES

LETTER

www.acsami.org

Water Desalination Using Carbon-Nanotube-Enhanced Membrane Distillation

Ken Gethard, Ornthida Sae-Khow, and Somenath Mitra*

Department of Chemistry and Environmental Science, New Jersey Institute of Technology, Newark, New Jersey 07102, United States

ABSTRACT: Carbon nanotube (CNT) enhanced membrane distillation is presented for water desalination. It is demonstrated that the immobilization of the CNTs in the pores of a hydrophobic membrane favorably alters the water−membrane interactions to promote vapor permeability while preventing liquid penetration into the membrane pores. For a salt concentration of 34 000 mg L^{-1} and at 80 °C, the nanotube incorporation led to 1.85 and 15 times increase in flux and salt reduction, respectively.

KEYWORDS: desalination, membrane distillation, carbone nanotubes, membrane separation

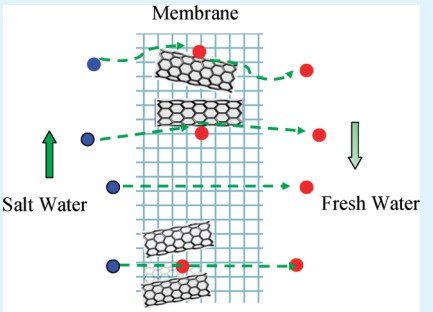

Desalination by Carbon Nanotube Enhanced Membrane Distillation

INTRODUCTION

Membrane distillation (MD) is a water purification process where a heated aqueous solution is passed through the lumen of a porous hydrophobic hollow fiber. While preventing the transport of the liquid phase, MD relies on the net flux of water vapor from the warm to the cool side of the membrane. Typically, MD is carried out at 60−90 °C, which is significantly lower than conventional distillation. Therefore, it has the potential to generate high-quality drinking water using only low-temperature heat sources such as waste heat from industrial processes and solar energy. In general, MD has received much attention as an alternative to thermal, chemical and reverse osmosis desalination of sea and brackish waters.[1−6] The driving force for mass transport in MD is provided by the vapor pressure difference across the membrane.[7] A key component in such a process is the membrane itself because it determines both flux and selectivity. As of now the throughput of MD processes are relatively low, and the development of novel membrane architecture is of great importance to enhance desalination via MD.

Recently, we have demonstrated that immobilizing CNTs in different types of membranes alter the solute-membrane interactions, which is one of the major physicochemical factors affecting the permeability and selectivity of a membrane. Referred to as carbon nanotube immobilized membrane (CNIM), here the CNTs serve as a sorbent and provide an additional pathway for solute transport. These membranes have been used in solvent extraction and pervaporation[8] and have demonstrated superior performance.[9] The objective of this research is to study the effect of CNTs on the enhancement in desalination efficiency via membrane distillation (MD).

EXPERIMENTAL DETAILS

The membrane modules for MD were constructed in a shell and tube format using 1/4 in. tubing and threaded brass pipe fittings. Thirty-six, 6-in. long hollow fiber strands were used in the module. Each module contained approximately 0.21 cm^2 of effective membrane contact area (based on fiber internal diameter). The ends were then sealed with epoxy to prevent leakage into the shell side. Vacuum was applied to one drain port to draw air through the other port, which created a higher pressure differential and provided a sweep air. Air flow was regulated at a rate of 1 L min^{-1}. The CNIM was prepared using Celgard type X-50 (Celgard, LLC, Charlotte, NC, USA) hollow fiber as the starting material. The process was as follows: ten milligrams of multiwall nanotubes (Cheap Tubes, Inc., Brattleboro, VT, USA) were dispersed in a solution containing 0.1 mg of polyvinylidene fluoride in 15 mL of acetone by sonicating for an hour. The PVDF/CNTs dispersion was forced under vacuum into the pore structure of the polypropylene membrane. The CNIM was produced during this step and the PVDF served as glue that held the CNTs in place. The membrane was flushed with acetone to remove excess CNTs and PVDF. Membrane morphology was studied using scanning electron microscopy (Leo, model 1550) and thermo gravimetric analysis (TGA) was performed using a Perkin-Elmer Pyris instrument.

The experimental system is shown in Figure 2. The salt mixture used in these experiments contained 88% NaCl and 12% $MgSO_4$. The solutions tested ranged from 10 to 34 000 mg L^{-1}. The water to be treated was pumped through the module using a HPLC pump. The solution traveled through a heat exchanger which allowed it to be heated to the desired temperature. As the solution traveled up the module, the permeate was discharged through the drain port and collected in a vacuum trap. The ionic strength of the original solution, the permeate and the concentrate were measured using an Oakton EC Testr 11+ multi range conductivity meter. All experiments were repeated in triplicate and the relative

Received: October 12, 2010
Accepted: December 13, 2010
Published: December 28, 2010

ACS Publications © 2010 American Chemical Society

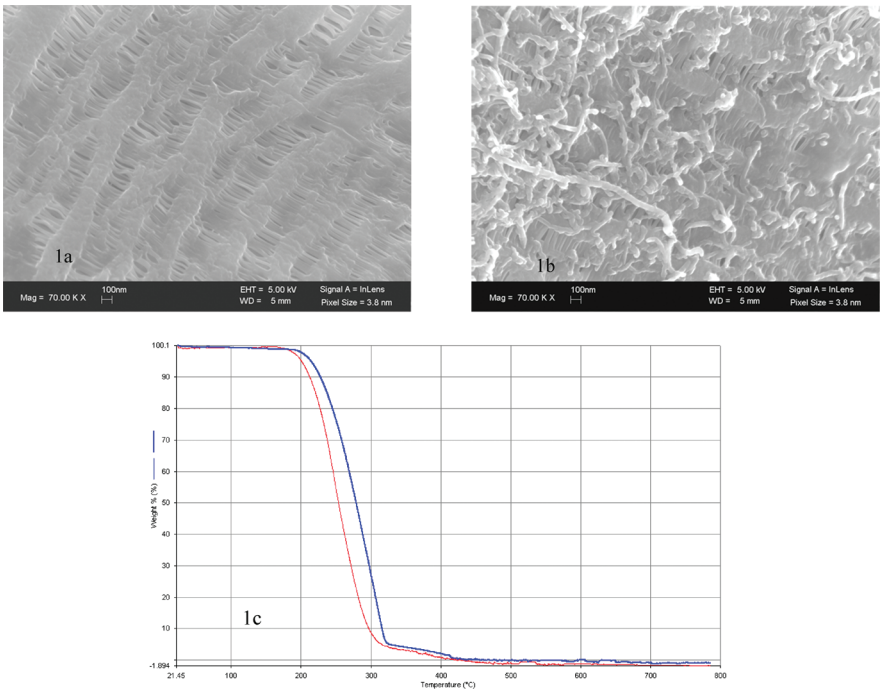

Figure 1. (a, b) SEM images of the original membrane and the CNIM. (c) Thermal gravitational analysis of the plain membrane and CNIM.

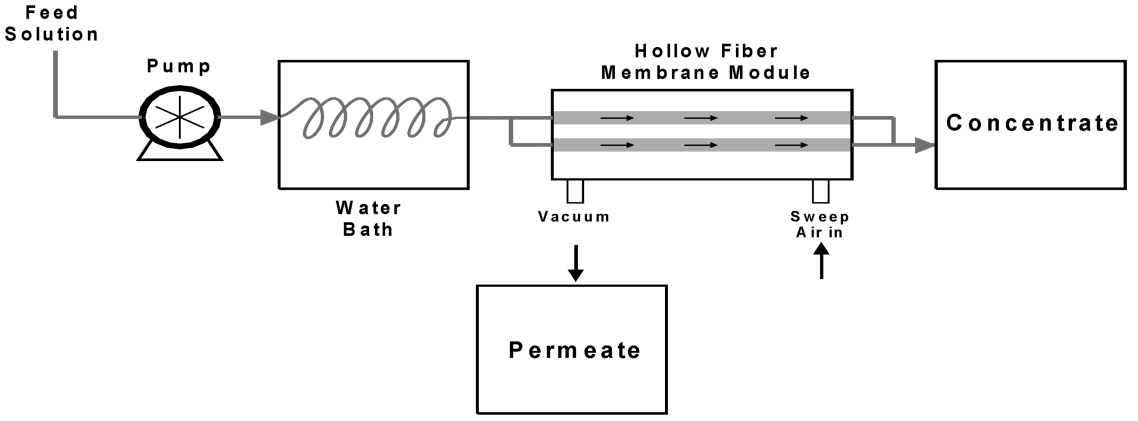

Figure 2. Schematic diagram of the experimental setup.

standard deviation of these measurements was found to be less than 5%.

RESULTS AND DISCUSSION

Scanning electron micrographs of the original membrane and CNIM are shown in images a and b in Figure 1. The incorporation of CNTs is clearly evident, and the CNTs were found to be uniformly distributed. The TGA is presented in Figure 1c. This indicated that the CNIM contained approximately 0.5% CNTs by weight. It was also observed the presence of CNTs enhanced the thermal stability of the membrane by increasing the onset of thermal degradation by as much as 29 °C. This is an important factor for MD, where the elevated temperatures can affect the membrane material.

The proposed mechanisms of permeation in the presence of CNTs are shown in Figure 3. Immobilizing the CNTs in the pores alters the water−membrane interactions, which is one of the major physicochemical factors affecting the permeability and selectivity of the membrane.[10] Because CNTs are highly hydrophobic, they decrease the tendency of a pore to become wet with liquid, so higher transport of pure vapor can occur. It is well-known that gas flow across a membrane pore follows Knudsen, Fickian, or molecular diffusion[11−13]. Because CNTs are known to have rapid sorption and desorption capacity,[14−16] it is possible they allow the water vapor molecules to follow a surface diffusion pattern, in which the solute hops from one site to another by interacting with the surfaces. This action may increase overall vapor transport. The CNTs can also provide an alternate route for fast mass transport via diffusion along their smooth surface[17,18]. The water vapor may also be transported directly through the inner tubes of the CNTs, which are known to enhance vapor transport.[19]

It is also well-established that CNTs have high thermal conductivity, which is a significant factor.[20] The higher thermal conductivity of the CNTs reduces the temperature gradient in the membranes, thus reducing condensation and allowing more

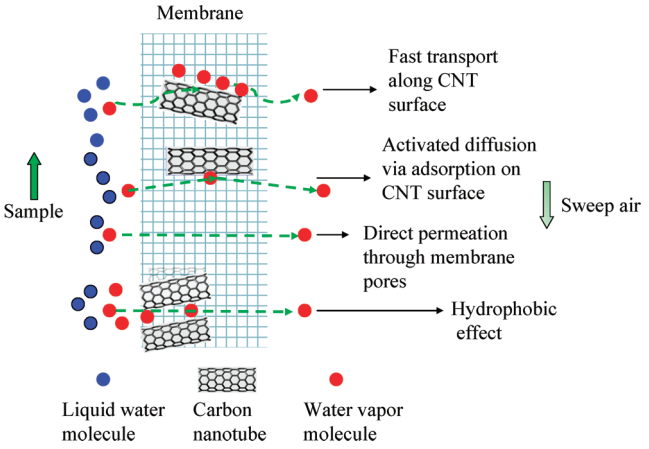

Figure 3. Mechanisms of MD in the presence of CNTs.

vapor to permeate through the pores. The condensation of water is known to reduce the hydrophobicity of the membrane leading to the attraction of more water molecules, which may eventually lead to pore clogging. The presence of CNTs reduces these effects. The relatively uniform temperature distribution leads to higher temperature in the permeate side of the membrane and lowers the surface tension[21] in the pores, thus allowing easier transport of water vapors.

MD experiments were carried out in the range of 60−100 °C. For both membrane types, the salt reduction and flux increased with temperature up to 80 °C. There was a leveling off and even slight reduction at higher temperatures. This data is shown is Figure 4a. The absolute level of salt reduction and flux per cm^2 of membrane was higher for CNIM at all temperatures. The incorporation of CNTs generated higher salt reduction and flux at significantly lower temperatures. The effect was most pronounced at lower temperatures. For example, at 60 °C and 0.5 mL min^{-1} feed flow, the salt reduction using CNIM was 6 times higher and was nearly the same as that accomplished at 90 °C using the conventional membrane. Both salt reduction and flux reached their peaks at 80 °C when the CNIM was used. The data demonstrate that CNIM can provide significantly higher eco-efficiency, because more pure water generation can be carried out at a significantly lower temperature.

Desalination as a function of flow rate is shown in Figure 4b when feed solution temperature was at 80 °C. In the flow rate range studied, in both cases, the salt reduction and flux per cm^2 of membrane decreased with flow rate. Compared to the conventional membrane, the CNIM demonstrated significantly higher flux and salt reduction at all feed flow rates. Flux doubled in the in the presence of CNTs and salt reduction increased five times. This is attributed to some of the reasons mentioned above, especially the fact that the CNTs serve as sorbent sites for vapor transport while rejecting the liquid water because of its high hydrophobicity. Improvement in salt reduction was observed at all flow rates, which ranged from 1.4 to 4.7 times higher. The ionic radius of Na^+ and Cl^- are 1.02 and 1.81 Å, respectively.[22] It is well-known that during reverse osmosis, water clusters exceeding four molecules can transport salt ions through the polymeric membrane.[23] Because the pores here are significantly larger (0.04 μm), the salt permeation in the membranes occurs mainly due to the entrainment of fine liquid droplets in the vapor phase. Therefore, it is concluded that the enhancement in salt reduction in the presence of the CNTs is due to the relatively higher vapor

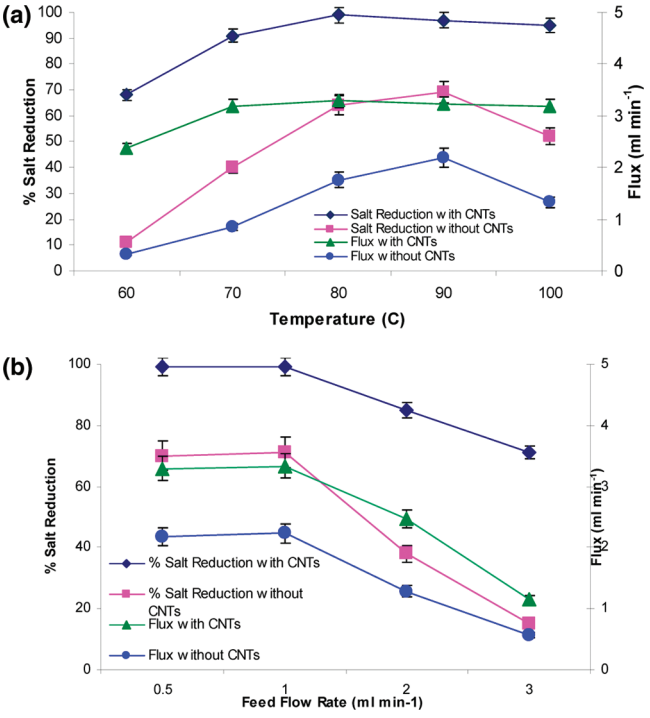

Figure 4. (a) Effect of temperature on salt reduction and flux at a feed flow rate of 0.5 mL min^{-1}; (b) effect of flow rate on salt reduction and flux at 80 °C.

flux and the rejection of water molecules due to higher hydrophobicity. The higher flux and salt reduction have practical ramifications because they lead to significantly higher efficiency processes. Higher salt reduction can be attained at higher flow rates, thus requiring less membrane material and energy per unit of water treated.

It is well-known that salt reduction in membrane processes decreases with increased salt concentration.[24,25] This was measured as a function of salt concentration and the data is presented in Table 1. The measurements were carried out at a flow rate of 0.5 mL min^{-1} and 80 °C. These measurements were made in triplicate and represent a relative standard deviation of less than 5%. The results showed a substantial decrease in flux (25%) for the plain membranes as the salt concentration was increased from 10 to 34 000 mg L^{-1}. This phenomenon has been reported before.[26,27] On the other hand, the CNIM showed no appreciable decrease in flux, most likely due to the hydrophobic nature of the CNTs, which prevented the liquid phase penetration into the membrane. Also, the salt reduction capability of CNIM was significantly higher at all concentrations. These varied from 99 to 15%, while in the plain membrane it was 71 to 1%. This indicates that the CNIM was less susceptible to salt bleed-through than the standard membrane. Once again, this is attributed to the CNIM's ability to selectively allow the passage of water vapor.

Mass Transfer in the Presence of Carbon Nanotubes. The water vapor flux J_w through the membrane is given by[28]

$$J_w = k(C^L - C^V) \quad (1)$$

where k is the mass transfer coefficient and C^L and C^V are the liquid and vapor-phase concentrations. C^L is the concentration of the exit stream (in mg L^{-1}) after the removal of the vapor phase,

Table 1. Salt Reduction and Flux at Different Feed Concentrations[a]

	membranes with CNTs		membranes without CNTs	
feed solution concentration (mg/L)	% salt reduction	total flux (mL cm^{-2} min^{-1})	% salt reduction	total flux(mL cm^{-2} min^{-1})
10	99	3.23	71	2.24
100	93	3.19	56	1.90
1000	32	3.28	13	2.00
10000	27	3.05	2	1.86
34000	15	3.09	1	1.67

[a] All measurements were at 80°C and at a feed flow rate of 0.5 mL min.

and C^V is the salt concentration in the condensed vapor phase. Ideally, the latter should be close to zero.

The reciprocal of k is the overall resistance to mass transfer and[29]

$$\frac{1}{k} = \frac{1}{k^L} + \frac{1}{k^M} + \frac{1}{k^V} \quad (2)$$

where $1/k^L$ is the liquid boundary layer resistance, $1/k^M$ is the membrane resistance, and $1/k^V$ is the permeate side boundary resistance. The liquid boundary layer resistance is dependent on parameters such as feed flow rate, viscosity, and density, which depend upon the salt concentration. Membrane resistance is a function of the membrane thickness, temperature, and the permeability of water vapor through the membrane. Permeate side boundary layer resistance is relatively small because the vapors are immediately removed. The flux through the membranes was calculated as

$$J = \frac{w^P}{tA} \quad (3)$$

where J is the flux, w^P is the total mass of permeate collected, t is the permeate collection time, and A is the membrane surface area. The overall mass transfer coefficient was calculated by

$$k = \frac{J}{c} \quad (4)$$

where, k is the mass transfer coefficient, J is the flux calculated from eq 3, and c is the feed solution concentration in mg L^{-1}.

The mass transfer coefficients at a flow rate of 0.5 mL min^{-1} and different temperatures are presented in Figure 5a, and were found to be 2−6 times higher in the presence of the CNTs. The effect of temperature on k was significantly more pronounced for the plain membrane where the increase was nearly 6 fold in the 60−80 °C range. This was attributed to an increase in the diffusion coefficient. In general, while diffusivity in the membrane increases with temperature, the sorption or the partition coefficient decreased. As a result of these two opposing effects, the overall increase in k was not as pronounced in the presence of the CNTs. Figure 5b shows the effect of flow rate (at 80 °C) on the mass transfer coefficient. At low flow rates, the overall mass transfer is controlled by diffusion through the boundary layer. Turbulence at high flow rates reduces the boundary layer effects, and at this point k is no longer a function of flow rate. The flattening of the profile was observed for the unmodified membrane but not the CNIM. As the flow rate of feedwater was increased from 0.5 to 1.0 mL min^{-1}, k in the unmodified membrane increased from 2.78×10^{-6} to 5.63×10^{-6} m/s, and stayed more or less constant beyond that point. Interestingly, the

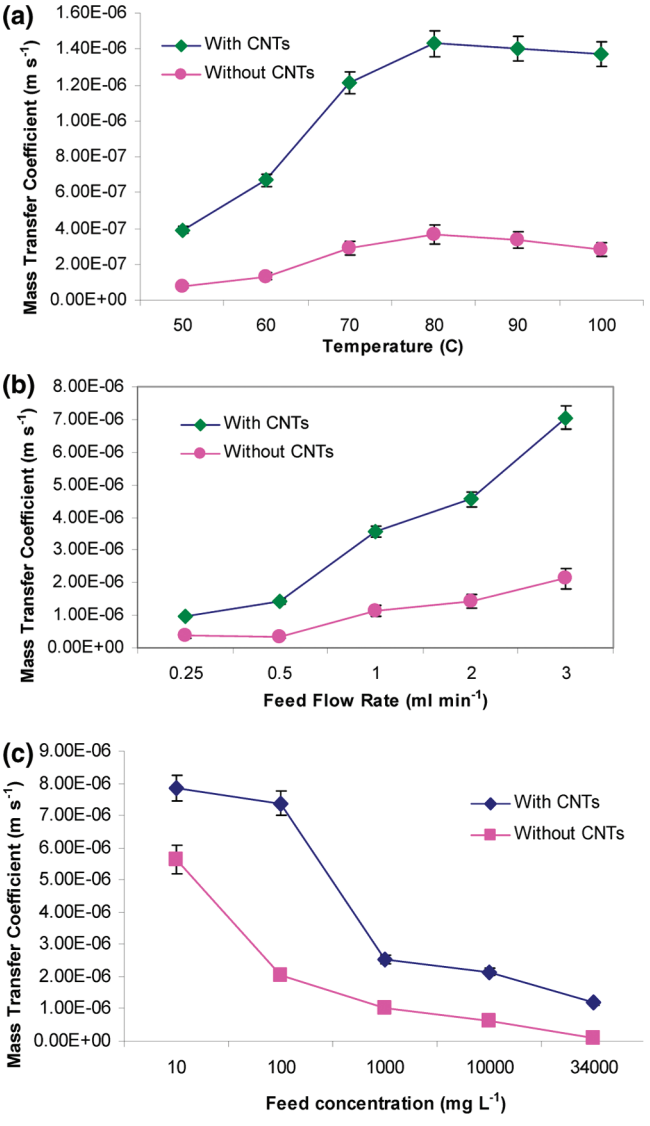

Figure 5. Mass transfer coefficients as a function of: (a) temperature at a feed flow rate 0.5 mL min^{-1}; (b) flow rate at 80 °C; (c) concentration at a flow rate of 0.5 mL min^{-1} and temperature of 80 °C.

overall mass transfer coefficient was less affected by the presence of the CNTs at low flow rates and the difference increased with flow rate. At a flow rate of 0.5 mL min^{-1}, the mass transfer coefficient of the CNIM was 1.4 times higher than the unmodified membrane, but increased to 2.7 times at 3 mL min^{-1}. In general, the presence of the CNTs led to enhanced permeability

through the membrane, and mass transfer was not limited by diffusion through the boundary layer even at high flow rates. The mass transfer coefficients as a function of inlet salt concentration at 80 °C and 0.5 mL min^{-1} are presented in Figure 5c. As expected, the values of k decreased with concentration, although they were consistently higher in the presence of CNTs. As compared to the plain membrane, in the salt concentration range of 10 to 10 000 mg L^{-1}, the mass transfer coefficients for the CNIM were higher by a factor of 1.4−3.5. At an inlet salt concentration of 34 000 mg L^{-1}, the CNIM represented a salt reduction that was higher by a factor of 15. This indicates that even at this extreme concentration, the CNIM selectively allowed the passage of water vapor and minimized salt permeation.

CONCLUSIONS

The advantages of CNIM compared to conventional MD include significantly higher flux and salt reduction for a wide range of salt concentrations up to the equivalent of seawater. Another advantage is that the CNIM can facilitate membrane distillation at a relatively lower temperature, higher flow rate, and salt concentration. Compared to a plain membrane, the CNIM demonstrated the same level of salt reduction at a 20 °C lower temperature, and at a flow rate that was six times higher. Together, these lead to a more efficient process which could potentially make MD economically competitive with existing desalination technologies.

AUTHOR INFORMATION

Corresponding Author
*E-mail: mitra@njit.edu. Tel.: 001 (973) 5965611.

ACKNOWLEDGMENT

We acknowledge the support of Celgard LLC for their contribution of membrane material.

REFERENCES

(1) Peng, P.; Fane, A. G.; Li, X. *Desalination* **2005,** *173*, 45–54.
(2) Wirth, D.; Cabassud, C. *Desalination* **2003,** *47*, 139–145.
(3) Evans, L. R.; Miller J. E. *Sweeping Gas Membrane Desalination Using Commercial Hydrophobic Hollow Fiber Membranes*; Report SAND2002-0138 ; Sandia National Laboratories: Albuquerque, NM, 2002.
(4) *Desalination Water Purification Research and Development Program Report No. 81*; College of Engineering, University of Texas at El Paso: El Paso, TX, 2004.
(5) Babu, B. R.; Rastogi, N. K.; Raghavarao, K. S. *J. Membr. Sci.* **2008,** *322*, 146–153.
(6) Banat, F.; Jumah, R.; Garaibeh, M. *Renewable Energy* **2001,** *25*, 293–305.
(7) Popov, V. N. *Mater. Sci. Eng., A* **2004,** *43*, 61–102.
(8) Sae-Khow, O.; Mitra, S. *Anal. Chem.* **2010,** *82*, 5561–5567.
(9) Sae-Khow, O.; Mitra, S. *J. Phys. Chem. C* **2010,** *114*, 16351–16356.
(10) Polotskaya, G. A.; Penkova, A. V.; Toikka, A. M. *Desalination* **2006,** *200*, 400–402.
(11) Alves, V. D.; Coelhoso, I. M. *J. Membr. Sci.* **2004,** *228*, 159–167.
(12) Alboy, S.; Broadbett, L.; Snorr, R. *AIChE J.* **2006,** *52*, 3679–3687.
(13) Gilrong, J.; Soffer, A. *J. Membr. Sci.* **2002,** *209*, 339–252.
(14) Hussain, C.; Mustansar, S.; Mitra, S. *Analyst* **2009,** *134*, 1928–1933.
(15) Dehouche, Z.; Lafi, L.; Grimard, N.; Goyette, J.; Chahine, R. *Nanotechnology* **2005,** *16*, 402–409.
(16) Staszczuk, P.; Blacnio, M.; Kowalska, E. *J. Therm. Anal. Calorim.* **2006,** *86*, 245–253.
(17) Striolo., A. *Nano Lett.* **2006,** *6*, 633–639.
(18) Thomas, J. A.; McGaughey, A. J. H. *Nano Lett.* **2008,** *8*, 2788–2793.
(19) Fujiwara, A.; Ishii, K.; Suematsu, K.; Kautaura, H.; Maniwa, Y.; Suzuki, S.; Achiba, Y. *Chem. Phys. Lett.* **2001,** *336*, 205–211.
(20) Hone, J.; Whitney, M.; Piskoti, C.; Zettl, A. *Phys. Rev. B: Condens. Matter Mater. Phys.* **1999,** *15*, 2514–2516.
(21) McElroy, J. P. *J. Colloid Interface Sci.* **1979,** *72*, 147–149.
(22) Burgess, J. *Ions in Solution: Basic Principals of Chemical Interactions*; Ellis Horwood: Chichester, U.K., 1988; Chapter 4 .
(23) Strathmann, H.; Michaels, A. S. *Desalination* **1977,** *28*, 195–202.
(24) Zhou, W.; Song, L. *Environ. Sci. Technol.* **2005,** *39*, 3382–3387.
(25) Meltzer, T. *Pharmaceutical Water Systems*; Tall Oaks Publishing: Littleton, CO, 1996; Chapter 9.
(26) Voros, N. G.; Maroulis, D.; Marinos-Kouris, D. *Desalination* **1996,** *104*, 141–154.
(27) *FILMTEC Membranes−Factors Affecting RO Membrane Performance*; Dow form 609−00055−498XQRP ; Dow Chemical: Midland, MI, 1998.
(28) Dutta, K.; Sikdar, S. K. *Environ. Sci. Technol.* **1999,** *33*, 1709–1716.
(29) Vane, L. M.; Alavarez, F. R.; Mullins, B. *Environ. Sci. Technol.* **2001,** *35*, 391–397.